Journal of Nuclear Medicine, published on January 27, 2022 as doi:10.2967/jnumed.121.263371

Synthesis and Preclinical Evaluation of ^{177}Lu-labeled Radiohybrid PSMA Ligands (rhPSMAs) for Endoradiotherapy of Prostate Cancer

Alexander Wurzer[#1], Jan-Philip Kunert[#1], Sebastian Fischer[1], Veronika Felber[1], Roswitha Beck[1], Francesco de Rose[2], Calogero D'Alessandria[2], Wolfgang Weber[2] and Hans-Jürgen Wester[1]

1 Chair of Pharmaceutical Radiochemistry, Technical University of Munich, Garching, Germany.

2 Department of Nuclear Medicine, Klinikum rechts der Isar, Technical University of Munich, Munich, Germany.

# contributed equally

Corresponding author:

Alexander Wurzer, PhD

Phone: +49.89.289.12203

Fax: +49.89.289.12204

Email: Alexander.Wurzer@tum.de

Technical University of Munich,

Chair of Pharmaceutical Radiochemistry,

Walther-Meißner-Str. 3

85748 Garching

GERMANY

rhPSMA for therapy of prostate cancer

ABSTRACT

Introduction: The prostate-specific membrane antigen (PSMA)-targeted radiohybrid (rh) ligand [^{177}Lu]Lu-rhPSMA-7.3 has recently been assessed in a pretherapeutic dosimetry study in prostate cancer patients. In comparison to [^{177}Lu]Lu-PSMA I&T, application of [^{177}Lu]Lu-rhPSMA-7.3 resulted in a significantly improved tumor dose, but also higher kidney accumulation. **Aim:** Although rhPSMA-7.3 has been initially selected as the lead compound for diagnostic application based on the characterization of its gallium complex, a systematic comparison of the most promising ^{177}Lu-labeled rhPSMA ligands is still missing. Thus, this study aimed to identify the rhPSMA ligand with most favorable pharmacokinetics for ^{177}Lu-radioligand therapy.

Methods: The four isomers of [^{177}Lu]Lu-rhPSMA-7 (namely [^{177}Lu]Lu-rhPSMA-7.1, -7.2, -7.3 and -7.4), along with the novel radiohybrid ligands [^{177}Lu]Lu-rhPSMA-10.1 and -10.2, were compared to the state-of-the-art compounds [^{177}Lu]Lu-PSMA I&T and [^{177}Lu]Lu-PSMA-617. The comparative evaluation comprised affinity studies (IC_{50}) and internalization experiments on LNCaP cells, as well as lipophilicity measurements. In addition, we determined the apparent molecular weight (AMW) of each tracer as a parameter for human serum albumin (HSA) binding. Biodistribution studies and µSPECT imaging was performed in LNCaP-tumor bearing mice at 24 h post injection.

Results: ^{177}Lu-labeling of the radiohybrids was carried out according to the established procedures for the currently established PSMA-targeted ligands. All ligands showed potent binding to PSMA-expressing LNCaP cells, with affinities in the low nanomolar range and high internalization rates. Surprisingly, most pronounced differences were identified regarding the HSA-related AMW. While [^{177}Lu]Lu-rhPSMA-7 isomers demonstrated the highest AMW and thus strongest HSA-interactions, [^{177}Lu]Lu-rhPSMA-10.1 showed an AMW lower than [^{177}Lu]Lu-rhPSMA-7.3 but higher than the ^{177}Lu-labeled references PSMA I&T and PSMA-617. In biodistribution studies [^{177}Lu]Lu-rhPSMA-10.1 exhibited the lowest kidney uptake and fastest excretion from the blood pool of all rhPSMA ligands, while preserving a high tumor accumulation.

Conclusion: Clinical investigation of [^{177}Lu]Lu-rhPSMA-10.1 is highly warranted in order to determine if the favorable pharmacokinetics observed in mice will also result in high tumor uptake and decreased absorbed dose to kidneys and other non-target tissues in patients.

Radiohybrid, rhPSMA, PSMA, Radioligand Therapy, Prostate Cancer

INTRODUCTION

Radioligand therapy (RLT) of metastatic castration resistant prostate cancer (mCRPC) with ligands targeting prostate-specific membrane antigen (PSMA) holds great promise for patients who exhausted conventional treatment regimens. Currently ^{177}Lu-labeled PSMA-617 (*1*) and PSMA I&T (*2*) are the most-extensively evaluated agents in this class and have demonstrated favorable safety and good treatment response rates (*3,4*). Although regulatory approval is still awaited for both agents, their application in compassionate use programs has recently been reaffirmed by the European Association of Nuclear Medicine procedure guidelines for ^{177}Lu-PSMA therapy (*5*). [^{177}Lu]Lu-PSMA-617 has been evaluated by Novartis in a phase 3 clinical trial (NCT 03511664) in patients with mCRPC. Here, [^{177}Lu]Lu-PSMA-617 was compared to the best standard of care. The investigators recently announced that both primary endpoints of overall and radiographic progression-free survival were met (*6*). In addition, an ongoing phase 3 trial investigating [^{177}Lu]Lu-PSMA I&T (NCT 04647526), is evaluating its efficacy versus abiraterone or enzalutamide in delaying radiographic progression in patients with mCRPC after second-line hormonal treatment. Retrospective clinical comparison of ^{177}Lu-labeled PSMA-617 and PSMA I&T point towards nearly identical pharmacokinetics of both tracers and clinical efficacy is assumed to be similar with no clear advantage of either compound (*7*).

Recently, the novel class of radiohybrid (rh) PSMA-targeted ligands was introduced by our group (*8*). These compounds combine a Silicon-Fluoride-Acceptor (SiFA) for ^{19}F/^{18}F-isotopic exchange radiolabeling and a chelator for complexation of a (radio)metal (e.g. ^{177}Lu, ^{68}Ga or ^{225}Ac). Respective ligand pairs of "**^{18}F**/non-radioactive metal" and "^{19}F/**radiometal**", e.g. [^{18}F]Lu-rhPSMA and [^{177}Lu]Lu-rhPSMA are chemically identical and thus display identical pharmacokinetics, offering unique possibilities for theranostic applications (Figure 1).

For prostate cancer diagnosis, the first clinical evaluations were conducted with the ^{18}F-labeled ^{nat}Ga-chelate of rhPSMA-7, which demonstrated a favorable biodistribution and indicated a high diagnostic performance for N-staging and localization of biochemical recurrence in patients with prostate cancer (*9-11*). Since rhPSMA-7 was found to be composed of four diastereoisomers (rhPSMA-7.1, -7.2, -7.3, -7.4), a

preclinical selection process was initiated which identified [^{18}F]Ga-rhPSMA-7.3 (often abbreviated as ^{18}F-rhPSMA-7.3) as the novel diagnostic lead compound (*12*) for current phase 3 clinical trials (NCT04186819, NCT04186845).

For initial evaluation of the radiohybrid technology for therapeutic applications, rhPSMA-7.3 was labeled with Lu-177 and compared to [^{177}Lu]Lu-PSMA I&T in biodistribution and dosimetry studies in mice. Both ligands showed a similar uptake in healthy organs, resulting in a similar dose to all major organs including bone marrow and kidney (*13*). Compared with [^{177}Lu]Lu-PSMA I&T, [^{177}Lu]Lu-rhPSMA-7.3 exhibited a 2.8- and 4.7-fold higher tumor uptake at 1 and 168 h post-injection (p.i), respectively, resulting in a significantly higher dose at the tumor and a superior treatment response (*13*).

In a pretherapeutic comparative dosimetry study of ^{177}Lu-labeled rhPSMA-7.3 and PSMA I&T in a small patient cohort (n=6, intraindividual comparison) an approximately 2.4-fold higher mean absorbed dose for tumor lesions of the radiohybrid ligand was found consistent with the pre-clinical observations (*14*). However, contradictory to animal studies, the mean absorbed dose to different healthy organs was also higher, e.g. 2.3-fold higher doses to kidneys and 2.2-fold higher doses to the bone marrow for [^{177}Lu]Lu-rhPSMA-7.3 versus [^{177}Lu]Lu-PSMA I&T. The authors concluded that the radiohybrid tracer holds promise for similar therapeutic effects as obtained with [^{177}Lu]Lu-PSMA I&T, while offering potential economic advantages by ~2-fold reduction of the injected radioactive doses (*14*).

The selection of rhPSMA-7.3 as lead compound for diagnostic application was based on the evaluation of gallium-chelates [^{18}F]Ga-rhPSMA-7.1, -7.2, -7.3 and -7.4 (*12*). Since it is known from literature that the complex structure of the metal-chelate (e.g. [Ga]DOTAGA and [Lu]DOTAGA; DOTAGA: 2-(4,7,10-tris(carboxymethyl)-1,4,7,10-tetraazacyclododecan-1-yl)pentanedioic acid)) within a radioligand can influence its pharmacokinetic properties (*15,16*), all ^{177}Lu-labeled isomers of rhPSMA-7 have been included in this comparison. The isomers differ in the stereoconfiguration of the diaminopropionic acid branching unit (*D*-Dap or *L*-Dap) and the glutamic acid arm at the DOTA-GA-chelator (*R*- or *S*-DOTA-GA [DOTA-GA: 2-(4,7,10-tris(carboxymethyl)-1,4,7,10-tetraazacyclododecan-1-

yl)pentanedioic acid]: rhPSMA-**7.1** (*D*-Dap–*R*-DOTA-GA), rhPSMA-**7.2** (*L*-Dap–*R*-DOTA-GA), rhPSMA-**7.3** (*D*-Dap–*S*-DOTA-GA), rhPSMA-**7.4** (*L*-Dap–*S*-DOTA-GA).

Given the promising initial data from ^{177}Lu-labeled rhPSMA-7.3, the aim of the present study was to evaluate whether other isomers of ^{177}Lu-labeled rhPSMA-7 or the closely-related compounds, [^{177}Lu]Lu-rhPSMA-10.1 (*D*-Dap) and -10.2 (*L*-Dap) (where DOTA [(1,4,7,10-tetraazacyclododecane-1,4,7,10-tetraacetic acid)] replaces the DOTA-GA chelator) might have further improved biodistributon kinetics in normal organs whilst maintaining the high tumour uptake found with [^{177}Lu]Lu-rhPSMA-7.3. We evaluated the ligands in comparison with reference ligands, [^{177}Lu]Lu-PSMA-617 and [^{177}Lu]Lu-PSMA I&T (Figure 2) *in vitro* (lipophilicity, IC_{50}, internalization into LNCaP cells, binding to human serum albumin (HSA)) and in biodistribution studies in LNCaP tumor-bearing mice.

MATERIALS AND METHODS

A detailed description on the chemical synthesis of rhPSMA and the analytical instruments is provided in the supplemental information.

Radiolabeling

Radiolabeling with no-carrier added Lu-177 was performed according to the established procedures for PSMA-targeted ligands (*1*,*2*). Briefly, the precursor (1.0 nmol, 10 µL, 0.1 mM in DMSO) was added to 10 µL of 1.0 M aqueous NaOAc buffer (pH 5.5). Subsequently, 20 to 50 MBq [^{177}Lu]$LuCl_3$ (Specific Activity > 3000 GBq/mg at the time of radiolabeling, 740 MBq/mL, 0.04 M HCl, ITM, Garching, Germany) was added and the mixture filled up to 100 µL with 0.04 M HCl. The reaction mixture was heated for 20-30 min at 90°C and the radiochemical purity (RCP) determined using radio-HPLC and radio-TLC with 0.1 M sodium citrate buffer on iTLC-SG chromatography paper (Agilent, Santa Clara, USA) and 1.0 M NH_4OAc/DMF buffer (1/1; *v*/*v*) on TLC Silica gel 60 F_{254} plates (Merck Millipore, Burlington, USA).

Lipophilicity

Approximately 1 MBq of the ^{177}Lu-labeled PSMA ligand was dissolved in 1 mL of a 1:1 mixture (*v*/*v*) of phosphate-buffered saline (PBS, pH 7.4) and *n*-octanol (n=6). After vigorous mixing of the suspension for 3 min, the vial was centrifuged at 15000×g for 3 min and 100 µL aliquots of both layers were measured in a γ-counter. Finally, the ratio of the radioactivity detected in the *n*-octanol sample and the PBS buffer was calculated and expressed as distribution ratio log $D_{7.4}$.

Binding to HSA

Binding of ^{177}Lu-labeled ligands to HSA was assessed by albumin mediated size exclusion chromatography (AMSEC), a novel method that has recently been developed by our group to determine the apparent molecular weight (AMW) of a compound in the presence of HSA. A dedicated and detailed description of the AMSEC method will be published elsewhere to cover the context and the development process of this method in its entirety. Briefly, a gel filtration size exclusion column (Superdex 75 Increase 10/300 GL, fractionation range 70 – 3 kDa, GE Healthcare, Uppsala, Sweden) was calibrated as recommended by the manufacturer using a commercially available set of proteins (Gel Filtration LMW Calibration Kit, GE Healthcare, Buckinghamshire, UK). AMSEC experiments were carried out by injection of the various radioligands using an HSA buffer at physiological concentration (Biowest, Nuaillé, France) as mobile phase at room temperature. Depending on the strength of the HSA/ligand interaction during the chromatographic procedure, an injected radioligand (1.0 MBq, 10-20 GBq/µmol) can show a reduced retention time that correlates to AMWs higher than the actual, physical molecular weight (the latter being for all investigated ligands <2 kDa, and thus below the column fractionation range). The stronger this interaction, the longer the mean time the ligand is bound to HSA during the chromatographic process and the faster the ligand is eluted from the column. By means of calibration, the retention time can be translated into a ligand-specific AMW (expressed in kDa) as a parameter allowing quantification of the extent of HSA binding. The detection window ranges between 2.1 kDa (cut-off value, determined [^{18}F]fluoride; no HSA

interaction) and 70.2 kDa (experimental molecular weight of HSA; maximum HSA interaction). [^{177}Lu]Lu-rhPSMA-7.3 served as an internal standard during AMSEC studies (30.4 ± 0.5 kDa; n=10).

Affinity Determinations (IC_{50}) and Internalization Studies

Competitive binding studies were determined on LNCaP cells (1.5×10^5 cells in 0.25 mL/well) after incubation at 4°C for 1 h, using (((*S*)-1-carboxy-5-(4-([^{125}I]iodo)benzamido)pentyl)carbamoyl)-*L*-glutamic acid ([^{125}I]IBA)KuE; 0.2 nM/well) as reference radioligand (n=3). Internalization studies of the radiolabeled ligands (1.0 nM/well) were performed on LNCaP cells (1.25×10^5 cells in 0.25 mL/well) at 37°C for 1 h and accompanied by ([^{125}I]IBA)KuE (0.2 nM/well), as reference. Data were corrected for non-specific binding and normalized to the specific internalization observed for the reference (n=3), as previously published (*8*).

***In Vivo* Experiments**

All animal experiments were conducted in accordance with general animal welfare regulations in Germany (German animal protection act, as amended on 18.05.2018, Art. 141 G v. 29.3.2017 I 626, approval no. 55.2-1-54-2532-71-13) and the institutional guidelines for the care and use of animals. LNCaP tumor xenografts were established in 6-8 week-old male CB-17 severe combined immunodeficient (SCID) mice as described previously (*8*).

Biodistribution Studies. The ^{177}Lu-labeled PSMA ligands (2-5 MBq; 0.1 nmol) were injected under isoflurane anesthesia into the tail vein of mice that were sacrificed 24 h p.i.(n = 4-5). Selected organs were removed, weighed, and measured in a γ-counter. All rhPSMA ligands were evaluated during the same time period (Q1/2020), whereas ^{177}Lu-labeled PSMA-617 and PSMA I&T (*17*) were assessed in 2016, using the identical cell line, mouse model and experimental procedure.

µSPECT/CT Imaging. Static images of ^{177}Lu-labeled ligands in sacrificed mice were recorded 24 h p.i. directly after blood collection, with an acquisition time of 45 min using the HE-GP-RM collimator and a stepwise multi-planar bed movement. For imaging studies, a VECTor4 small-animal SPECT/PET/OI/CT from MILabs (Utrecht, Netherlands) was applied. Data were reconstructed using the MILabs-Rec software

(version 10.02) and PMOD4.0 software (PMOD TECHNOLOGIES LLC, Zurich, Switzerland). After imaging, mice were subjected to biodistribution studies.

RESULTS

Synthesis and Radiolabeling

Uncomplexed PSMA ligands were obtained via a solid phase/solution phase synthetic strategy with chemical purities >97% as determined by HPLC (absorbance at 220 nm). Identity was confirmed by mass spectrometry. Complexation with 2.5-fold molar excess $LuCl_3$ lead to quantitative formation of the respective Lu-PSMA ligands, which were used for *in vitro* studies. ^{177}Lu-labeling of PSMA ligands according to standard manual procedures resulted in a RCP >95%, determined by radio-HPLC and radio-TLC (see Supplemental table 1).

In Vitro Characterization

Results of the *in vitro* evaluation of all rhPSMAs and the reference ligands PSMA-617 (*1*) and PSMA I&T (*2*) are summarized in Figure 3 and Supplemental table 2. PSMA binding affinity (IC_{50}; Figure 3, A) was high and in the low nanomolar range for all Lu-rhPSMA ligands (range: 2.8±0.5 to 3.6±0.6 nM) and the two reference ligands (Lu-PSMA I&T: 4.2±0.8 nM, Lu-PSMA-617: 3.3±0.2 nM).

Slight differences between the ligands were found for the PSMA-mediated internalization into LNCaP cells (1 h, 37°C), which is expressed as a percentage of the specific internalization of the reference ligand ([^{125}I]IBA)KuE (Figure 3B). While [^{177}Lu]Lu-rhPSMA-7.1 and [^{177}Lu]Lu-PSMA I&T showed the lowest internalization rates with values of 137±6% and 145±14%, respectively, the other rhPSMA compounds showed an approximately 1.4-fold higher internalization (range: 177±15 to 206±8%), similar to that of [^{177}Lu]Lu-PSMA-617 (203±10%).

The ^{177}Lu-labeled rhPSMA-7 isomers as well as the references [^{177}Lu]Lu-PSMA I&T and [^{177}Lu]Lu-PSMA-617 demonstrated a high and similar hydrophilicity, expressed as a partition-coefficient (log $D_{7.4}$; *n*-

octanol and PBS pH 7.4) with values between -4.1±0.1 and -4.3±0.3. The DOTA-conjugates [^{177}Lu]Lu-rhPSMA-10.1 and -10.2, showed a slightly lower hydrophilicity with a log $D_{7.4}$ of -3.8 (Figure 3C).

The AMW of the tracers was determined to compare the relative HSA-binding strength of the ligands. Exemplary chromatograms of AMSEC experiments showing ligand-specific retention times are provided in Supplemental figures 1-3. Interestingly, remarkable differences were found for the AMWs of the state-of-the-art references and even among the single isomers of ^{177}Lu-labeled rhPSMA-7 and rhPSMA-10, respectively (Figure 3D). While [^{177}Lu]Lu-PSMA I&T showed the lowest HSA interaction (AMW=5.3 kDa) followed by [^{177}Lu]Lu-PSMA-617 (AMW=13.7 kDa), all radiohybrid ligands demonstrated an at least 1.5-fold higher AMW with values between 21.8 and 35.7 kDa. Among the radiohybrids, the two DOTA-conjugates [^{177}Lu]Lu-rhPSMA-10.1 and -10.2 showed the lowest AMW (25.1 kDa and 21.8 kDa), respectively, while *D*-Dap-configured [^{177}Lu]Lu-rhPSMA-7.1 (MW=26.3 kDa) and [^{177}Lu]Lu-rhPSMA-7.3 (MW=30.4kDa) showed the lowest AMWs within the rhPSMA-7 series (AMWs of *L*-Dap-comprising isomers: [^{177}Lu]Lu-rhPSMA-7.2 = 31.7 kDa and [^{177}Lu]Lu-rhPSMA-7.4 = 35.7 kDa).

In Vivo Characterization

Biodistribution studies. Overall, the comparative biodistribution study of the ^{177}Lu-labeled PSMA-ligands in LNCaP tumor-bearing mice at 24 h p.i. revealed a quite similar distribution pattern with high tumor uptake, fast excretion from background organs, but varying degree of activity retention in the kidneys (Figure 4, Supplemental table 3 and 4).

At 24 h p.i., the highest activity retention in the kidneys was found for [^{177}Lu]Lu-PSMA I&T (34.7±17.2%ID/g), whereas [^{177}Lu]Lu-PSMA-617 (1.4±0.4%ID/g) and [^{177}Lu]Lu-rhPSMA-10.1 (2.0±0.8%ID/g) demonstrated fastest renal clearance. Kidney uptake of the former lead compound [^{177}Lu]Lu-rhPSMA-7.3 was found to be 9.8±2.7 %ID/g, thus showing slower renal clearance than [^{177}Lu]Lu-rhPSMA-7.1 (4.1±0.8%ID/g), [^{177}Lu]Lu-rhPSMA-10.1 (2.0±0.8%ID/g) and [^{177}Lu]Lu-rhPSMA-10.2 (8.1±1.7%ID/g). These differences are also well illustrated in the µSPECT/CT images (see Figure 5). Tumor uptake was highest for all [^{177}Lu]Lu-rhPSMA-7 isomers and in the range of 11.6-12.7%ID/g, followed by

[^{177}Lu]Lu-rhPSMA-10.2 (10.5±3.3%ID/g) and -10.1 (9.8±0.3%ID/g), whereas the references ^{177}Lu-labeled PSMA-617 (7.5±0.9%ID/g) and PSMA I&T (4.1±1.1%ID/g) exhibited a lower tumor uptake.

Tumor-to-organ ratios. Interestingly, all radiohybrid ligands are cleared from the blood pool and background tissues with a kinetic profile that more resembles that of small molecules than that of larger proteins - despite their extensive binding to HSA. Amongst all radiohybrids, the highest tumor/blood and tumor/kidney ratio was found for [^{177}Lu]Lu-rhPSMA-10.1 (T/blood: 11498, T/kidney: 5.7), followed by [^{177}Lu]Lu-rhPSMA-7.1 (T/blood: 5971, T/kidney: 3.2), whereas [^{177}Lu]Lu-rhPSMA-7.3 showed inferior values (T/blood: 3843, T/kidney: 1.2). While [^{177}Lu]Lu-PSMA I&T (T/Blood: 408; T/Kidney: 0.2) exhibited rather slow excretion in mice, [^{177}Lu]Lu-PSMA-617 showed the highest tumor-to-kidney ratio (T/Blood: 1424; T/Kidney: 5.9), whereas its tumor-to-blood ratio was lower compared with all radiohybrid ligands (Supplemental table 5 and 6).

DISCUSSION

Although it has recently been demonstrated in patients that the uptake of [^{177}Lu]Lu-rhPSMA-7.3 in tumor lesions was on average 2- to 3-fold higher compared with [^{177}Lu]Lu-PSMA I&T, the slower clearance resulted in a comparatively higher dose to the kidney as organ at risk (*14*). In retrospect, this result is hardly surprising, since the selection process of the best diagnostic rhPSMA-7 isomer was based on criteria that are considered suboptimal for therapy: Fast blood clearance to reach high tumor/background ratios at early time points, predominantly renal clearance with high kidney retention to ensure low appearance of activity in the bladder at early time points. In contrast, the selection criteria for the best therapeutic isomer are different. Compared to today's therapeutic ligands, a slightly delayed blood clearance is preferred. The ligand should be excreted renally, while showing almost no retention in the kidneys. It must also be taken into account that the change in the isotope (Lutetium for RLT instead of Gallium for the diagnostic compound) results in a different structure and charge at the chelate–metal complex (Ga-DOTA: hexadentate, zwitterionic; Lu-DOTA: octadentate, uncharged) (*15*). This matter obviously influences the

pharmacokinetic properties of the entire ligand, as demonstrated by the prolonged clearance kinetics of the ^{177}Lu-labeled ´best diagnostic isomer´ rhPSMA-7.3 in patients (*14*).

With the aim to address these therapeutic criteria and to identify a ^{177}Lu-labeled rhPSMA tracer with more favorable characteristics for RLT, we carried out a co-evaluation of six different rhPSMA ligands (four rhPSMA-7 isomers and two rhPSMA-10 isomers) and compared the results with preclinical data of the two reference compounds PSMA-617 and PSMA I&T.

All Lu-complexed radiohybrid tracers and the external references, PSMA I&T and PSMA-617, demonstrated potent binding to LNCaP cells with an excellent affinity in the low nanomolar range and high internalization rates, which did not allow prioritization of certain candidates for further evaluation.
In the context of PSMA-targeted RLT, the kidney followed by the bone marrow are still considered the main organs at risk and uptake in these should be carefully considered (*18*).

In our comparative biodistribution studies pronounced differences in kidney uptake values were observed. Whereas our internal reference *D*-Dap-*S*-DOTAGA-configured [^{177}Lu]Lu-rhPSMA-7.3 showed a kidney uptake of 9.8±2.7 %ID/g at 24 h p.i., the uptake of the *D*-Dap-DOTA derivative [^{177}Lu]Lu-rhPSMA-10.1 reached only 20% of that value (2.0±0.8 %ID/g). Moreover, the stereoconfiguration of the Dap-branching unit (*D*-Dap or *L*-Dap) also resulted in a pronounced different kidney uptake, as shown for [^{177}Lu]Lu-rhPSMA-7.1 (*D*-Dap: 4.1±0.8%ID/g) and the 5-fold higher value of the corresponding *L*-Dap version [^{177}Lu]Lu-rhPSMA-7.2 (19.0±4.5%ID/g). As already demonstrated in a previous study of [^{18}F]Ga-rhPSMA ligands (*12*), these results impressively demonstrate once more that even small modifications in the arene binding region of PSMA-targeted ligands can have a remarkable influence on the biodistribution. In this former study the modification of the stereoconfiguration of the Dap branching unit and the DOTAGA-chelator resulted in superior pharmacokinetics of [^{18}F]Ga-rhPSMA-7.3 in mice compared to the diasteriomeric mixture [^{18}F]Ga-rhPSMA-7. This result was confirmed in patient studies, revealing a 5-fold

lower excretion of [^{18}F]Ga-rhPSMA-7.3 into the bladder, a 1.6-fold lower kidney uptake and a 1.6-fold higher tumor uptake compared to the diasteriomeric mixture [^{18}F]Ga-rhPSMA-7 (*19*).

Even though the results of our preclinical comparison are highly promising, there are many examples in the literature that question the direct transferability of the preclinical results to the clinical studies, particularly with regard to kidney clearance and kidney retention. The low kidney uptake of [^{177}Lu]Lu-PSMA-617 (1.4±0.4%ID/g at 24 h p.i.) in mice has often been highlighted as a major selection criteria that promoted its rapid clinical development and thus considered as major advantage compared to [^{177}Lu]Lu-PSMA I&T (kidney uptake: 34.7±17.2%ID/g at 24 h p.i.) (*20*). However, in contrast to preclinical results, head-to-head comparison of both ligands in patients has impressively demonstrated a nearly identical kidney uptake and clearance kinetic of both tracers (*7*). Moreover, a very similar absorbed dose to the kidney was found in dosimetry studies, [^{177}Lu]Lu-PSMA-617: 0.4±0.2 to 0.8±0.3 Gy/GBq (*21-23*); [^{177}Lu]Lu-PSMA I&T: 0.7±0.2 Gy/GBq (*24*). Until further investigations improve our understanding on species-dependent renal handling of PSMA tracers and in the absence of alternative and more valid selection criteria, the evaluation of the biodistribution in mice, including the assessment of the different excretion behavior, will remain our only viable option – although we should treat such data with appropriate caution.

Regarding important non-target organs like liver, muscle and heart, all ligands demonstrated almost identical and complete clearance 24 h p.i. Even though only low activity levels were found in the blood pool for all ligands, [^{177}Lu]Lu-rhPSMA-10.1 showed the best clearance of all investigated PSMA ligands, which is also expressed by the highest tumor-to-blood ratio (T/blood: 11498): 3-times higher value compared to [^{177}Lu]Lu-rhPSMA-7.3 and 8-times higher when compared to [^{177}Lu]Lu-PSMA-617.

The tendency of both DOTA-conjugated [^{177}Lu]Lu-rhPSMA-10 isomers for faster clearance can at least in part be explained by the HSA-binding experiments and our newly introduced in vitro parameter “AMW”. The molecular weight of a molecule is known to have a direct implication on the glomerular sieving coefficient (as a rule of thumb: the lower the molecular weight, the higher the glomerular sieving coefficient (GSC) and the faster excretion kinetics) (*25*). Thus, the stronger the interaction of a molecule with HSA or the higher the ratio [ligand $_{\text{bound to HSA}}$] / [ligand $_{\text{free}}$], the less ligand is subjected to glomerular filtration and

thus the less ligand is excreted. In our assay, this ratio is indirectly determined by calculating the AMW of each compound (details on these methods will be described elsewhere).

Looking at the AMW of ^{177}Lu-labeled PSMA-617 (13.7 kDa) and PSMA-I&T (5.3 kDa) as key reference points, the 2.3-fold lower AMW of PSMA I&T appears prima facie unproportional: Kulkarni et al. could demonstrate that [^{177}Lu]Lu-PSMA-617 exhibits only a marginally slower clearance in patients when compared to [^{177}Lu]Lu-PSMA I&T (*7*). However, taking into account the non-linear correlation of the molecular weight and GSC and the tiny changes of the GSC at low molecular weights, the differences in AMW of PSMA I&T and PSMA-617 result in only slightly different GSCs, which explains the similar kidney excretion kinetics of these two ligands in patients (*25*). In contrast, the higher AMW of [^{177}Lu]Lu-rhPSMA-7.3 (MW=30.4) would translate into a markedly lower GSC and thus a delayed clearance, which has been confirmed by clinical results from Feuerecker *et al. (14)*. Based on these results, we expect that the blood clearance kinetics of [^{177}Lu]Lu-rhPSMA-10.1 and -10.2 in humans will be somewhere between that of [^{177}Lu]Lu-rhPSMA-7.3 and [^{177}Lu]Lu-PSMA-617/PSMA-I&T. As demonstrated by Feuerecker *et al. (14)*, the remarkable tumor uptake of [^{177}Lu]Lu-rhPSMA-7.3 that has been found in our preclinical experiments (*13*) could also be observed in patients (effective dose of [^{177}Lu]Lu-rhPSMA-7.3: 6.4±6.7 mGy/MBq versus [^{177}Lu]Lu-PSMA I&T: 2.6±2.4 mGy/MBq). Thus, we are optimistic to be able to obtain a similar improved tumor uptake in patients during the clinical assessment of [^{177}Lu]Lu-rhPSMA-10.1 and thus tumor doses higher than those currently obtained with the state-of-the art non-hybrid ligands (*14*).

Certainly there are also other effects determining different clearance kinetics of radiopharmaceuticals in mice and men that must be considered, e.g. species differences in drug binding to serum albumin (*26*), different magnitude and binding affinities of the tracers to other plasma proteins than HSA, like alpha-1-acid glycoprotein (*27*), transthyretin (*28*) or lipoproteins (*29*). Moreover, individual differences in uptake of PSMA-ligands into the kidneys (*30*), varying relative proportions of hepatobiliary to renal clearance, and effects of species differences between mice and men must be taken into account. In summary, however, we are optimistic that the promising biodistribution profile of [^{177}Lu]Lu-rhPSMA-10.1

observed in mice together with its low AMW will translate as improved tumor doses and tumor/kidney dose ratios of this isomer in patients.

CONCLUSION

Based on this preclinical comparison, [^{177}Lu]Lu-rhPSMA-10.1 seems to be a very promising lead for the clinical development of a rhPSMA-targeted ligand for RLT. [^{177}Lu]Lu-rhPSMA-10.1 could have the potential to outperform the *in vivo* characteristics of the currently developed state-of-the-art PSMA targeted radioligands [^{177}Lu]Lu-PSMA-617 and [^{177}Lu]Lu-PSMA-I&T in men. Clinical studies are required to demonstrate whether our newly introduced, additional preclinical selection criteria, the AMW, could be a valuable parameter for the future development of further therapeutic radiopharmaceuticals with optimally adjusted clearance kinetics.

DISCLOSURE

HJW, AW, JPK, SF, VF are listed as inventors in patent applications for some therapeutic rhPSMA. HJW receives funding from the SFB 824 (Deutsche Forschungsgemeinschaft, Bonn, Germany, Sonderforschungsbereich 824, Project B11 and Z). HJW is founder, shareholder and scientific advisor of Scintomics GmbH, Fuerstenfeldbruck, Germany. WW is consultant for Blue Earth Diagnostics Ltd. No other potential conflicts of interest relevant to this article exist.

ACKNOWLEDGMENTS

The authors thank C.Turnbull for carefully proofreading the manuscript.

KEY POINTS

Question: Which ^{177}Lu-labeled rhPSMA ligand shows the best characteristics for radioligand therapy of prostate cancer?

Pertinent Findings: In preclinical experiments [^{177}Lu]Lu-rhPSMA-10.1 demonstrates a fast clearance kinetics from healthy tissues while preserving a high tumor uptake.

Implications for Patient Care: Preclinical data indicate more favorable pharmacokinetics for [^{177}Lu]Lu-rhPSMA-10.1 compared to [^{177}Lu]Lu-PSMA-617 and [^{177}Lu]Lu-PSMA-I&T for radioligand treatment, which has to be investigated in prospective clinical studies.

REFERENCES

1. Benesova M, Schafer M, Bauder-Wust U, et al. Preclinical evaluation of a tailor-made DOTA-conjugated PSMA inhibitor with optimized linker moiety for imaging and endoradiotherapy of prostate cancer. *J Nucl Med.* 2015;56:914-920.

2. Weineisen M, Schottelius M, Simecek J, et al. 68Ga- and 177Lu-labeled PSMA I&T: Optimization of a PSMA-targeted theranostic concept and first proof-of-concept human Studies. *J Nucl Med.* 2015;56:1169-1176.

3. Heck MM, Tauber R, Schwaiger S, et al. Treatment outcome, toxicity, and predictive factors for radioligand therapy with (177)Lu-PSMA-I&T in metastatic castration-resistant prostate cancer. *Eur Urol.* 2019;75:920-926.

4. Hofman MS, Violet J, Hicks RJ, et al. [(177)Lu]-PSMA-617 radionuclide treatment in patients with metastatic castration-resistant prostate cancer (LuPSMA trial): a single-centre, single-arm, phase 2 study. *Lancet Oncol.* 2018;19:825-833.

5. Kratochwil C, Fendler WP, Eiber M, et al. EANM procedure guidelines for radionuclide therapy with (177)Lu-labelled PSMA-ligands ((177)Lu-PSMA-RLT). *Eur J Nucl Med Mol Imaging.* 2019;46:2536-2544.

6. Morris MJ, Bono JSD, Chi KN, et al. Phase III study of lutetium-177-PSMA-617 in patients with metastatic castration-resistant prostate cancer (VISION). *J Clin Oncol.* 2021;39:LBA4-LBA4.

7. Kulkarni HR, Singh A, Schuchardt C, et al. PSMA-based radioligand therapy for metastatic castration-resistant prostate cancer: The Bad Berka experience Since 2013. *J Nucl Med.* 2016;57:97s-104s.

8. Wurzer A, Di Carlo D, Schmidt A, et al. Radiohybrid ligands: a novel tracer concept exemplified by (18)F- or (68)Ga-labeled rhPSMA inhibitors. *J Nucl Med.* 2020;61:735-742.

9. Kroenke M, Wurzer A, Schwamborn K, et al. Histologically confirmed diagnostic efficacy of (18)F-rhPSMA-7 PET for N-staging of patients with primary high-risk prostate cancer. *J Nucl Med.* 2020;61:710-715.

10. Eiber M, Kroenke M, Wurzer A, et al. (18)F-rhPSMA-7 PET for the detection of biochemical recurrence of prostate cancer after radical prostatectomy. *J Nucl Med.* 2020;61:696-701.

11. Oh SW, Wurzer A, Teoh EJ, et al. Quantitative and qualitative analyses of biodistribution and PET image quality of a novel radiohybrid PSMA, (18)F-rhPSMA-7, in patients with prostate cancer. *J Nucl Med.* 2020;61:702-709.

12. Wurzer A, Parzinger M, Konrad M, et al. Preclinical comparison of four [(18)F, (nat)Ga]rhPSMA-7 isomers: influence of the stereoconfiguration on pharmacokinetics. *EJNMMI Res.* 2020;10:149.

13. Yusufi N, Wurzer A, Herz M, et al. Comparative preclinical biodistribution, dosimetry, and endoradiotherapy in metastatic castration-resistant prostate cancer using (19)F/(177)Lu-rhPSMA-7.3 and (177)Lu-PSMA I&T. *J Nucl Med.* 2021;62:1106-1111.

14. Feuerecker B, Chantadisai M, Allmann A, et al. Pre-therapeutic comparative dosimetry of (177)Lu-rhPSMA-7.3 and (177)Lu-PSMAI&T in patients with metastatic castration resistant prostate cancer (mCRPC). *J Nucl Med.* 2021 Sep 16;jnumed.121.262671, Epub ahead of print.

15. Wadas TJ, Wong EH, Weisman GR, Anderson CJ. Coordinating radiometals of copper, gallium, indium, yttrium, and zirconium for PET and SPECT imaging of disease. *Chem Rev.* 2010;110:2858-2902.

16. Umbricht CA, Benešová M, Schmid RM, et al. (44)Sc-PSMA-617 for radiotheragnostics in tandem with (177)Lu-PSMA-617-preclinical investigations in comparison with (68)Ga-PSMA-11 and (68)Ga-PSMA-617. *EJNMMI Res.* 2017;7:9.

17. Wirtz M, Schmidt A, Schottelius M, et al. Synthesis and in vitro and in vivo evaluation of urea-based PSMA inhibitors with increased lipophilicity. *EJNMMI Res.* 2018;8:84.

18. Yordanova A, Becker A, Eppard E, et al. The impact of repeated cycles of radioligand therapy using [(177)Lu]Lu-PSMA-617 on renal function in patients with hormone refractory metastatic prostate cancer. *Eur J Nucl Med Mol Imaging.* 2017;44:1473-1479.

19. Oh SW, Wurzer A, Yusufi N, et al. Preclinical dosimetry and human biodistribution of 18F-rhPSMA-7 and 18F-rhPSMA-7.3. *J Nucl Med.* 2019;60:1635-1635.

20. Wester HJ, Schottelius M. PSMA-targeted radiopharmaceuticals for imaging and therapy. *Semin Nucl Med.* 2019;49:302-312.

21. Delker A, Fendler WP, Kratochwil C, et al. Dosimetry for (177)Lu-DKFZ-PSMA-617: a new radiopharmaceutical for the treatment of metastatic prostate cancer. *Eur J Nucl Med Mol Imaging.* 2016;43:42-51.

22. Kabasakal L, Toklu T, Yeyin N, et al. Lu-177-PSMA-617 prostate-specific membrane antigen inhibitor therapy in patients with castration-resistant prostate cancer: Stability, bio-distribution and dosimetry. *Mol Imaging Radionucl Ther.* 2017;26:62-68.

23. Violet J, Jackson P, Ferdinandus J, et al. Dosimetry of (177)Lu-PSMA-617 in metastatic castration-resistant prostate cancer: Correlations between pretherapeutic imaging and whole-body tumor dosimetry with treatment outcomes. *J Nucl Med.* 2019;60:517-523.

24. Okamoto S, Thieme A, Allmann J, et al. Radiation dosimetry for (177)Lu-PSMA I&T in metastatic castration-resistant prostate cancer: Absorbed dose in normal organs and tumor lesions. *J Nucl Med.* 2017;58:445-450.

25. Norden AG, Lapsley M, Lee PJ, et al. Glomerular protein sieving and implications for renal failure in Fanconi syndrome. *Kidney Int.* 2001;60:1885-1892.

26. Colclough N, Ruston L, Wood JM, MacFaul PA. Species differences in drug plasma protein binding. *MedChemComm.* 2014;5:963-967.

27. Smith SA, Waters NJ. Pharmacokinetic and pharmacodynamic considerations for drugs binding to alpha-1-acid glycoprotein. *Pharm Res.* 2018;36:30.

28. Buxbaum JN, Reixach N. Transthyretin: the servant of many masters. *Cell Mol Life Sci.* 2009;66:3095-3101.

29. Wasan KM, Brocks DR, Lee SD, Sachs-Barrable K, Thornton SJ. Impact of lipoproteins on the biological activity and disposition of hydrophobic drugs: implications for drug discovery. *Nat Rev Drug Discov.* 2008;7:84-99.

30. Begum NJ, Thieme A, Eberhardt N, et al. The effect of total tumor volume on the biologically effective dose to tumor and kidneys for (177)Lu-labeled PSMA peptides. *J Nucl Med.* 2018;59:929-933.

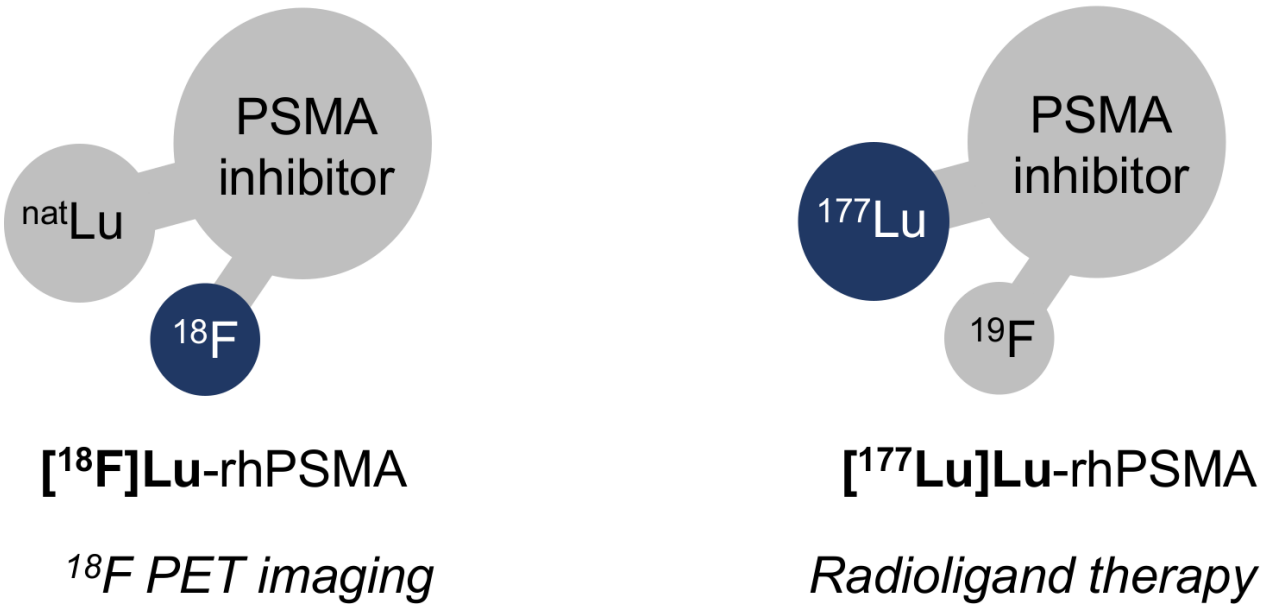

Figure 1: The theranostic radiohybrid concept applied to PSMA-targeted ligands. The molecules offer two labeling sites for radionuclides, a silicon-fluorine acceptor (SiFA) site for ^{18}F-labeling via isotopic exchange and a chelator for radiometallation. The ^{18}F-labeled cold lutetium complexed ligand ([^{18}F]Lu-rhPSMA) is chemically identical to the ^{177}Lu-labeled cold fluorine compound ([^{177}Lu]Lu-rhPSMA), therefore representing true theranostic agents for PET-imaging and radioligand therapy.

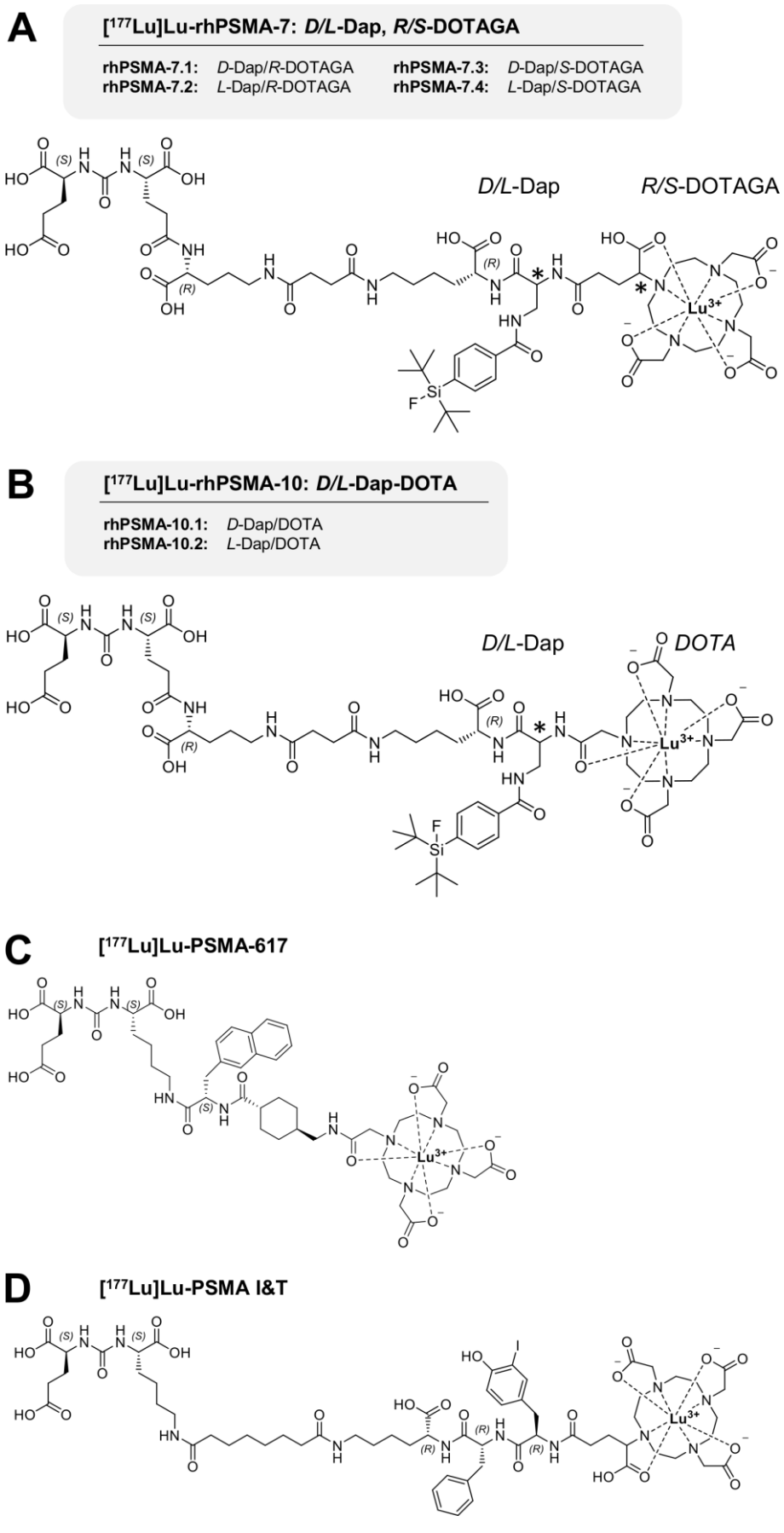

Figure 2: (A) The rhPSMA-7 isomers differ in the stereoconfiguration of the diaminopropionic acid branching unit (*D*-Dap or *L*-Dap) and the glutamic acid arm at the DOTA-GA-chelator (*R*- or *S*-DOTA-GA). (B) rhPSMA-10.1 (*D*-Dap) and rhPSMA-10.2 (*L*-Dap), both equipped with the DOTA chelator, also differ in the stereoconfiguration of the branching unit (*D*-Dap or *L*-Dap). The well-established PSMA-addressing ligands PSMA-617 (C) and PSMA I&T (D) served as reference compounds (*1*,*2*).

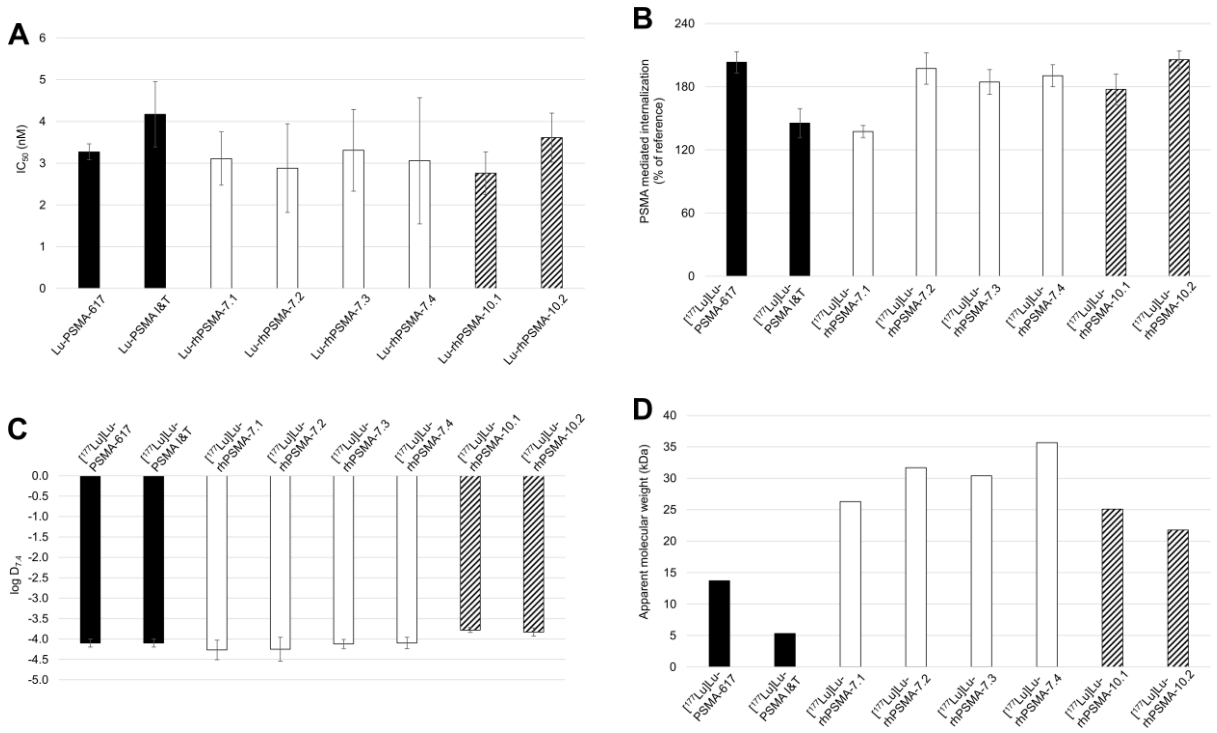

Figure 3: A) Binding affinities (IC_{50} [nM], 1 h, 4°C) of Lu-rhPSMA-7.1 to -7.4 (white; n=3), Lu-rhPSMA-10.1, -10.2 (black/white stripes; n=3) and the references Lu-PSMA-617 and Lu-PSMA-I&T (black; n=3); **B**) PSMA-mediated internalization of [^{177}Lu]Lu-rhPSMA-7.1 to -7.4 (white; n=3), [^{177}Lu]Lu-rhPSMA-10.1, -10.2 (black/white stripes; n=3) and the references [^{177}Lu]Lu-PSMA-617 and [^{177}Lu]Lu-PSMA I&T (black; n=3) by LNCaP cells (1 h, 37°C) as a percentage of the reference ligand ([^{125}I]IBA)KuE); **C**) lipophilicity of [^{177}Lu]Lu-rhPSMA-7.1 to -7.4 (white; n=6), [^{177}Lu]Lu-rhPSMA-10.1, -10.2 (black/white stripes; n=6) and the references [^{177}Lu]Lu-PSMA-617 and [^{177}Lu]Lu-PSMA I&T (black; n=6), expressed as partition coefficient (log $D_{7.4}$ in *n*-octanol/PBS pH 7.4); **D**) apparent molecular weight of [^{177}Lu]Lu-rhPSMA-7.1 to -7.4 (white), [^{177}Lu]Lu-rhPSMA-10.1, -10.2 (black/white stripes) and the references [^{177}Lu]Lu-PSMA-617 and [^{177}Lu]Lu-PSMA I&T (black), as determined by human serum albumin-mediated size exclusion chromatography.

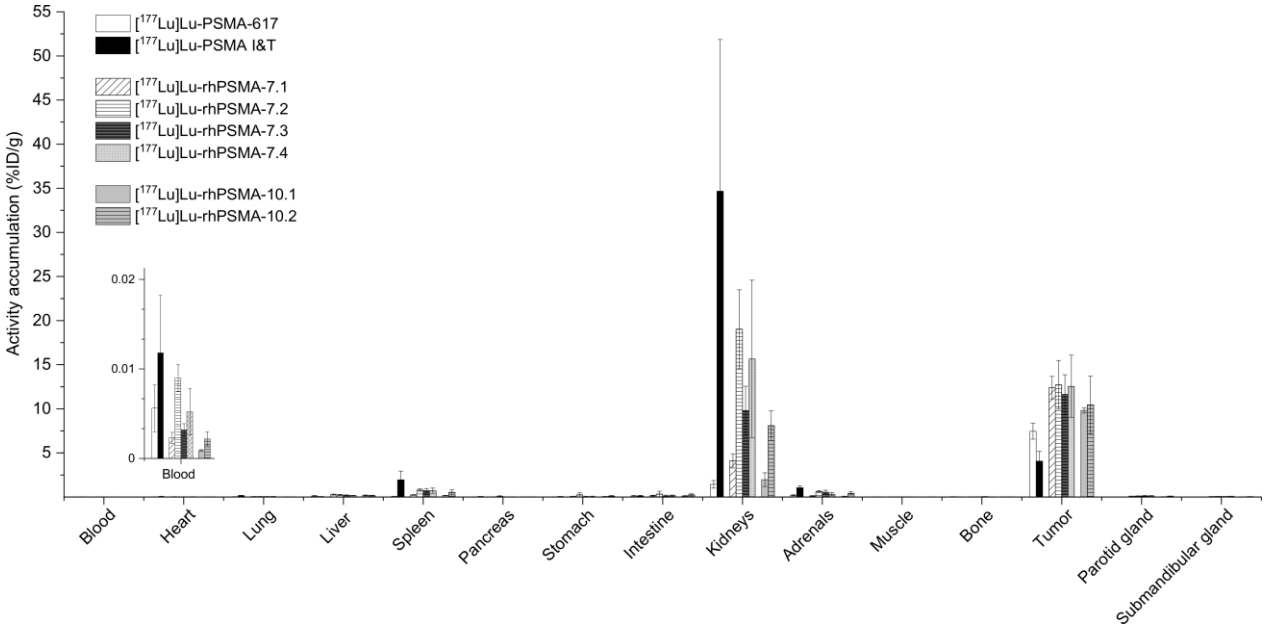

Figure 4: Biodistribution of [^{177}Lu]Lu-rhPSMA-7.1 to -7.4, [^{177}Lu]Lu-rhPSMA-10.1 and -10.2, and the references [^{177}Lu]Lu-PSMA-617 and [^{177}Lu]Lu-PSMA I&T at 24 h p.i. in male LNCaP tumor-bearing SCID mice. Data are expressed as a percentage of the injected dose per gram [%ID/g], mean ± standard deviation (n = 4−5). Values of [^{177}Lu]Lu-PSMA I&T were taken from a previously published study by our group (*17*) that has been carried out under identical conditions.

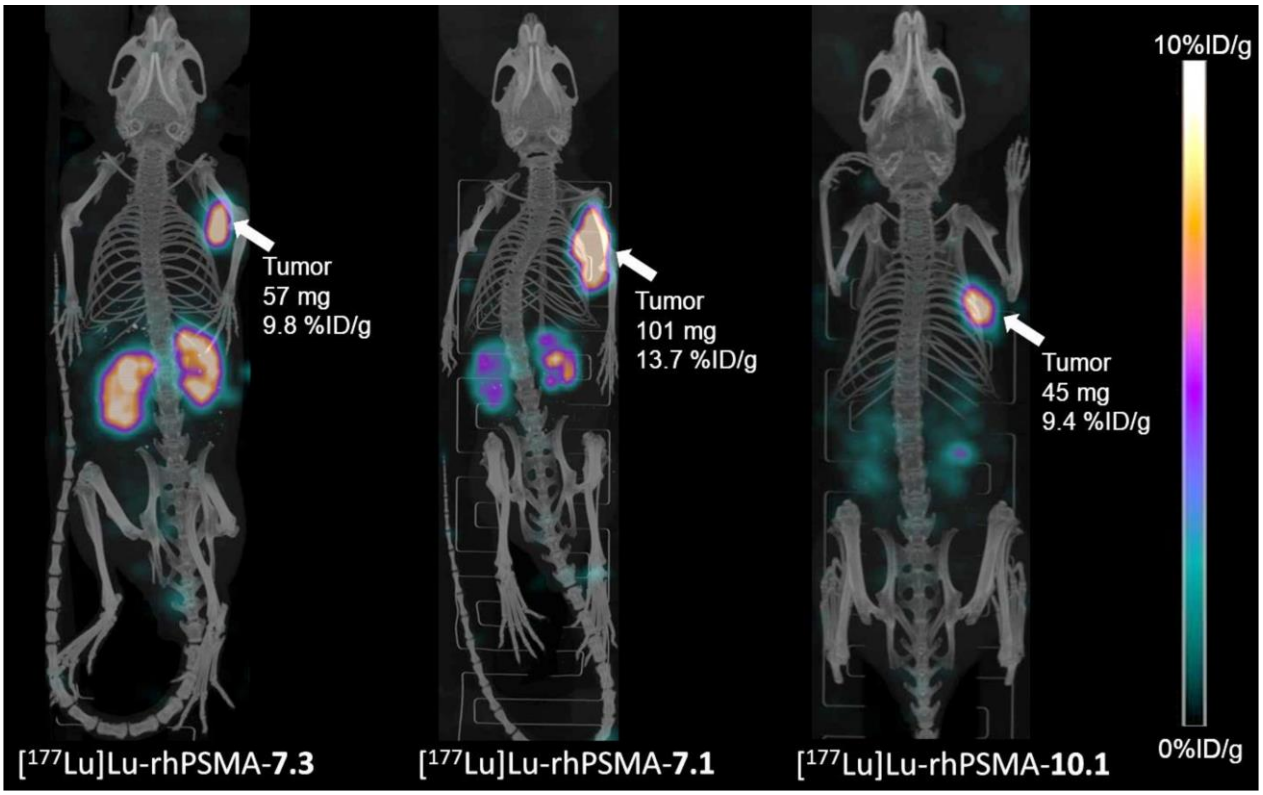

Figure 5: Static µSPECT/CT images (maximum intensity projections) of ^{177}Lu-labeled rhPSMA-7.3, rhPSMA-7.1 and rhPSMA-10.1 in LNCaP tumor-bearing mice, sacrificed 24 h p.i. and imaged directly after blood collection, with an acquisition time of 45 min on a VECTor4 small-animal SPECT/PET/OI/CT. Tumor weight and tracer uptake in the tumor (in percent of the injected dose/gram, [%ID/g]) were determined from subsequent biodistribution studies.

Graphical abstract:

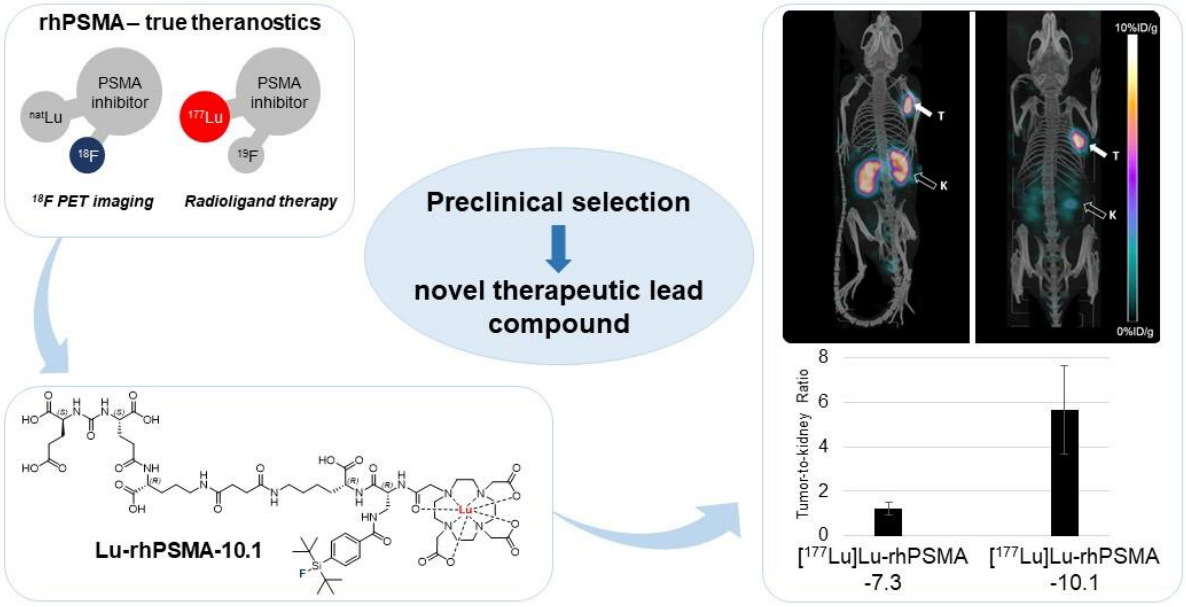

General Information

Analytical and preparative high-performance liquid chromatography (HPLC) was performed using Shimadzu gradient systems (Neufahrn, Germany) equipped with an SPD-20A UV/Vis detector. The columns for analytical (MultoKrom 100C18, 150×4.6 mm, 5 µm), radio-analytical (Multospher 100RP18, 125×4.6 mm, 5 µm) and preparative (MultoKrom 100C18, 250×20 mm, 5 µm) HPLC were purchased from CS Chromatographie Service (Langerwehe, Germany). Eluents for all HPLC operations were water (solvent A) and acetonitrile with 2 vol.% water (solvent B), both containing 0.1 vol.% trifluoroacetic acid (TFA). Radioactivity was detected via a HERM LB 500 NaI detector (Berthold Technologies, Bad Wildbad, Germany). Radio-thin layer chromatography (TLC) was carried out with a Scan-RAM detector (LabLogic Systems, Sheffield, United Kingdom). Electrospray ionization-mass spectra were acquired on an expression^{L} CMS (Advion, Harlow, UK).

Synthesis of PSMA Ligands

The uncomplexed radiohybrid ligands rhPSMA-7.1, -7.2, -7.3 and -7.4 were prepared by applying a mixed solid phase/solution phase synthetic strategy, according to the literature protocols (*1*). rhPSMA-10.1 and -10.2 were obtained in analogy to the rhPSMA-7 isomers, by substitution of the DOTA-GA chelator with DOTA. PSMA I&T was prepared according to the published procedure (*2*) and PSMA-617 was purchased from MedChemExpress LLC (Monmouth Junction, USA).

For complexation with non-radioactive lutetium for *in vitro* studies, a 2 mM solution of the PSMA inhibitor (1.0 eq.) in DMSO was combined with a 20 mM aqueous solution of $LuCl_3$ (2.5 eq.) and heated to 95°C for 30 min. Analytical data of the Lu-chelated PSMA ligands are summarized in the supporting information.

Analytical data of Lu-complexed PSMA inhibitors:

Lu-rhPSMA-7.1: RP-HPLC (10 to 70% B in 15 min): t_R = 9.7 min, K' = 3.85. Calculated monoisotopic mass ($C_{63}H_{96}FLuN_{12}O_{25}Si$): 1642.6; found: m/z = 1643.5 $[M+H]^+$, 822.5 $[M+2H]^{2+}$.

Lu-rhPSMA-7.2: RP-HPLC (10 to 70% B in 15 min): t_R = 9.4 min, K' = 3.70. Calculated monoisotopic mass ($C_{63}H_{96}FLuN_{12}O_{25}Si$): 1642.6; found: m/z = 1642.9 $[M+H]^+$, 822.0 $[M+2H]^{2+}$.

Lu-rhPSMA-7.3: RP-HPLC (10 to 70% B in 15 min)*: t_R* = 9.6 min*,* K' = 3.80*.* Calculated monoisotopic mass ($C_{63}H_{96}FLuN_{12}O_{25}Si$): 1642.6; found: m/z = 1643.4 $[M+H]^+$, 822.3 $[M+2H]^{2+}$.

Lu-rhPSMA-7.4: RP-HPLC (10 to 70% B in 15 min): t_R = 9.6 min*,* K' = 3.80*.* Calculated monoisotopic mass ($C_{63}H_{96}FLuN_{12}O_{25}Si$): 1642.6; found: m/z = 1643.0 $[M+H]^+$, 822.3 $[M+2H]^{2+}$.

Lu-rhPSMA-10.1: RP-HPLC (10 to 70% B in 15 min): t_R = 9.9 min, K' = 3.95. Calculated monoisotopic mass ($C_{60}H_{92}FLuN_{12}O_{23}Si$): 1570.6; found: m/z = 1571.8 $[M+H]^+$, 786.2 $[M+2H]^{2+}$.

Lu-rhPSMA-10.2: RP-HPLC (10 to 70% B in 15 min): t_R = 9.6 min, K' = 3.80. Calculated monoisotopic mass ($C_{60}H_{92}FLuN_{12}O_{23}Si$): 1570.6; found: m/z = 1571.9 $[M+H]^+$, 786.6 $[M+2H]^{2+}$.

Lu-PSMA-I&T: RP-HPLC (10 to 70% B in 15 min): t_R = 7.2 min, K' = 3.32. Calculated monoisotopic mass ($C_{63}H_{89}ILuN_{11}O_{23}$): 1669.5; found: m/z = 1670.5 $[M+H]^+$, 1113.8 $[2M+3H]^{3+}$.

Lu-PSMA-617: RP-HPLC (10 to 70% B in 15 min): t_R = 6.5 min, K' = 2.82. Calculated monoisotopic mass ($C_{49}H_{68}LuN_9O_{16}$): 1213.4; found: m/z = 1213.6 $[M+H]^+$, 607.5 $[M+2H]^{2+}$.

Supplemental Table 1: Radiochemical purity (RCP) of ^{177}Lu-labeled rhPSMA isomers, determined by radio-TLC before lipophilicity studies, using either the citrate buffer system (0.1 M sodium citrate buffer on iTLC-SG chromatography paper) or acetate buffer system (1.0 M NH_4OAc/DMF buffer (1/1; v/v) on TLC Silica gel 60 F254 plates).

[^{177}Lu]Lu-	**citrate-TLC RCP**	**acetate-TLC RCP**
rhPSMA-7.1	99.5%	99.7%
rhPSMA-7.2	99.8%	99.8%
rhPSMA-7.3	99.8%	99.9%
rhPSMA-7.4	99.8%	99.8%
rhPSMA-10.1	99.8%	99.8%
rhPSMA-10.2	99.7%	99.7%

Supplemental Table 2: Binding affinities (IC_{50} [nM], 1 h, 4°C) of Lu-rhPSMA-7.1 to -7.4 (n=3), Lu-rhPSMA-10.1, -10.2 (n=3) and the references Lu-PSMA-617 and Lu-PSMA-I&T (n=3); PSMA-mediated internalization of [^{177}Lu]Lu-rhPSMA-7.1 to -7.4 (n=3), [^{177}Lu]Lu-rhPSMA-10.1, -10.2 (n=3) and the references [^{177}Lu]Lu-PSMA-617 and [^{177}Lu]Lu-PSMA I&T (n=3) by LNCaP cells (1 h, 37°C) as a percentage of the reference ligand ([^{125}I]IBA)KuE); Lipophilicity of [^{177}Lu]Lu-rhPSMA-7.1 to -7.4 (n=6), [^{177}Lu]Lu-rhPSMA-10.1, -10.2 (n=6) and the references [^{177}Lu]Lu-PSMA-617 and [^{177}Lu]Lu-PSMA I&T (n=6), expressed as partition coefficient (log $D_{7.4}$) using the *n*-octanol/PBS (pH 7.4) distribution system ; Apparent molecular weight (AMW) of [^{177}Lu]Lu-rhPSMA-7.1 to -7.4, [^{177}Lu]Lu-rhPSMA-10.1, -10.2 and the references [^{177}Lu]Lu-PSMA-617 and [^{177}Lu]Lu-PSMA I&T, as determined by human serum albumin mediated size exclusion chromatography (AMSEC).

Compound	**[^{177}Lu]Lu-rhPSMA-7.1**	**[^{177}Lu]Lu-rhPSMA-7.2**	**[^{177}Lu]Lu-rhPSMA-7.3**	**[^{177}Lu]Lu-rhPSMA-7.4**	**[^{177}Lu]Lu-rhPSMA-**	**[^{177}Lu]Lu-rhPSMA-**	**[^{177}Lu]Lu-PSMA-617**	**[^{177}Lu]Lu-PSMA I&T**
IC_{50} [nM]	3.11 ± 0.64	2.88 ± 1.06	3.29 ± 1.00	3.06 ± 1.51	2.76 ± 0.51	3.61 ± 0.59	3.27 ± 0.19	4.17 ± 0.78
Internalization [%IBA-KuE]	137.4 ± 5.8	197.3 ± 15.0	184.4 ± 11.8	190.4 ± 10.5	177.4 ± 14.6	205.6 ± 8.3	203.2 ± 10.1	145.4 ± 13.8
log$D_{7.4}$	-4.27 ± 0.24	-4.25 ± 0.29	-4.12 ± 0.11	-4.10 ± 0.14	-3.78 ± 0.06	-3.83 ± 0.10	-4.1 ± 0.1	-4.1 ± 0.1
MW_{app} [kDa]	26.3	31.7	30.4	35.7	25.1	21.8	13.7	5.3

Supplemental Table 3: Biodistribution of [^{177}Lu]Lu-rhPSMA-7.1 to -7.4 at 24 h p.i. in male LNCaP tumor-bearing SCID mice. Data are expressed as a percentage of the injected dose per gram (% ID/g), mean ± standard deviation (SD; n=4).

	[^{177}Lu]Lu-rhPSMA-7.1 24 h p.i., n = 4		**[^{177}Lu]Lu-rhPSMA-7.2 24 h p.i., n = 4**		**[^{177}Lu]Lu-rhPSMA-7.3 24 h p.i., n = 4**		**[^{177}Lu]Lu-rhPSMA-7.4 24 h p.i., n = 4**	
uptake in % ID/g	**mean**	**SD**	**mean**	**SD**	**mean**	**SD**	**mean**	**SD**
blood	**0.0023**	**0.0006**	**0.0090**	**0.0015**	**0.0032**	**0.0007**	**0.0052**	**0.0026**
heart	0.036	0.009	0.032	0.005	0.031	0.009	0.032	0.006
lung	0.050	0.006	0.049	0.009	0.049	0.011	0.056	0.014
liver	**0.28**	**0.06**	**0.24**	**0.06**	**0.22**	**0.04**	**0.16**	**0.03**
spleen	0.24	0.04	0.79	0.13	0.73	0.23	0.72	0.29
pancreas	0.019	0.003	0.076	0.071	0.025	0.005	0.027	0.006
stomach	0.071	0.018	0.246	0.236	0.059	0.028	0.068	0.029
intestine	0.15	0.05	0.34	0.31	0.13	0.08	0.15	0.07
kidney	**4.10**	**0.81**	**19.04**	**4.45**	**9.82**	**2.74**	**15.66**	**8.92**
adrenals	0.12	0.04	0.61	0.13	0.56	0.22	0.34	0.18
muscle	0.011	0.001	0.010	0.002	0.009	0.003	0.010	0.003
bone	0.030	0.009	0.034	0.008	0.048	0.010	0.023	0.009
tumor	**12.40**	**1.27**	**12.73**	**2.76**	**11.63**	**2.24**	**12.56**	**3.52**
parotid gl.	0.083	0.020	0.114	0.030	0.131	0.042	0.111	0.057
submand. gl.	0.051	0.004	0.072	0.005	0.056	0.010	0.075	0.019

Supplemental Table 4: Biodistribution of [^{177}Lu]Lu-rhPSMA-10.1, -10.2 and the references [^{177}Lu]Lu-PSMA-617 and [^{177}Lu]Lu-PSMA I&T at 24 h p.i. in male LNCaP tumor-bearing SCID mice. Data are expressed as a percentage of the injected dose per gram (% ID/g), mean ± standard deviation (SD; n=4-5). Values of [^{177}Lu]Lu-PSMA I&T were taken from a previously published study by our group (*3*). N.d. not determined.

	[^{177}Lu]Lu-rhPSMA-10.1 24 h p.i., n = 5		**[^{177}Lu]Lu-rhPSMA-10.2 24 h p.i., n = 4**		**[^{177}Lu]Lu-PSMA-617 24 h p.i., n = 4**		**[^{177}Lu]Lu-PSMA-I&T 24 h p.i., n = 4**	
uptake in % ID/g	**mean**	**SD**	**mean**	**SD**	**mean**	**SD**	**mean**	**SD**
blood	**0.0009**	**0.0001**	**0.0022**	**0.0008**	**0.0056**	**0.0026**	**0.0118**	**0.0064**
heart	0.017	0.001	0.020	0.004	0.012	0.004	0.049	0.034
lung	0.032	0.004	0.036	0.007	0.039	0.013	0.158	0.029
liver	**0.18**	**0.06**	**0.15**	**0.05**	**0.12**	**0.06**	**0.05**	**0.01**
spleen	0.17	0.03	0.53	0.26	0.08	0.01	1.94	1.01
pancreas	0.013	0.002	0.021	0.002	0.011	0.004	0.048	0.029
stomach	0.056	0.014	0.104	0.069	0.020	0.003	0.048	0.021
intestine	0.11	0.05	0.24	0.13	0.12	0.08	0.12	0.06
kidney	**1.97**	**0.78**	**8.09**	**1.68**	**1.44**	**0.42**	**34.66**	**17.20**
adrenals	0.06	0.04	0.41	0.17	0.19	0.07	1.06	0.24
muscle	0.003	0.002	0.007	0.002	0.009	0.002	0.010	0.004
bone	0.022	0.008	0.020	0.008	0.027	0.017	0.014	0.004
tumor	**9.82**	**0.30**	**10.45**	**3.25**	**7.46**	**0.90**	**4.06**	**1.12**
parotid gl.	0.041	0.009	0.100	0.017	n.d.	n.d.	n.d.	n.d.
submand. gl.	0.037	0.007	0.046	0.009	n.d.	n.d.	n.d.	n.d.

Supplemental Table 5: Tumor-to-organ ratios of [^{177}Lu]Lu-rhPSMA-7.1 to -7.4 at 24 h p.i. in male LNCaP tumor-bearing SCID mice. Mean ± standard deviation (SD; n=4). Tumor-to-organ ratios were calculated from individual mice and mean values were determined.

	[^{177}Lu]Lu-rhPSMA-7.1 24 h p.i., n = 4		**[^{177}Lu]Lu-rhPSMA-7.2 24 h p.i., n = 4**		**[^{177}Lu]Lu-rhPSMA-7.3 24 h p.i., n = 4**		**[^{177}Lu]Lu-rhPSMA-7.4 24 h p.i., n = 4**	
tumor-to-organ ratio	**mean**	**SD**	**mean**	**SD**	**mean**	**SD**	**mean**	**SD**
blood	**5971**	**2358**	**1460**	**495**	**3843**	**1145**	**2570**	**820**
heart	368	122	409	125	394	82	387	81
lung	252	53	275	113	239	24	234	87
liver	**47**	**13**	**54**	**12**	**54**	**2**	**78**	**13**
spleen	54	13	16	3	17	3	19	4
pancreas	671	211	285	170	487	133	489	180
stomach	191	70	187	210	262	177	228	135
intestine	95	40	150	211	129	86	104	55
kidney	**3.2**	**0.9**	**0.7**	**0.2**	**1.2**	**0.3**	**1.0**	**0.5**
adrenals	119	54	21	1	23	7	43	14
muscle	1167	214	1453	623	1454	601	1269	92
bone	453	190	384	66	264	111	616	309
parotid gl.	163	69	112	14	93	21	99	13
submand. gl.	244	43	177	40	207	27	169	33

Supplemental Table 6: Tumor-to-organ ratios [^{177}Lu]Lu-rhPSMA-10.1, -10.2 and the references [^{177}Lu]Lu-PSMA-617 and [^{177}Lu]Lu-PSMA I&T at 24 h p.i. in male LNCaP tumor-bearing SCID mice. Mean ± standard deviation (SD; n=4-5). Values of [^{177}Lu]PSMA I&T were taken from a previously published study by our group (*3*). Tumor-to-organ ratios were calculated from individual mice and mean values were determined.

	[^{177}Lu]Lu-rhPSMA-10.1 24 h p.i., n = 5		**[^{177}Lu]Lu-rhPSMA-10.2 24 h p.i., n = 4**		**[^{177}Lu]Lu-PSMA-617 24 h p.i., n = 4**		**[^{177}Lu]Lu-PSMA-I&T 24 h p.i., n = 4**	
tumor-to-organ ratio	**mean**	**SD**	**mean**	**SD**	**mean**	**SD**	**mean**	**SD**
blood	**11498**	**1953**	**6125**	**4185**	**1424**	**455**	**408**	**209**
heart	568	52	585	321	704	270	128	77
lung	313	33	295	100	210	74	26	9
liver	**57**	**13**	**69**	**17**	**91**	**73**	**86**	**31**
spleen	58	11	27	19	93	22	3.0	2.0
pancreas	774	189	511	198	799	293	144	115
stomach	187	47	221	231	376	65	105	60
intestine	115	75	111	162	90	50	49	33
kidney	**5.7**	**2.0**	**1.4**	**0.6**	**5.9**	**3.0**	**0.15**	**0.08**
adrenals	171	111	33	22	44	15	4.1	1.5
muscle	2441	373	1798	792	855	279	496	242
bone	595	462	589	280	472	378	315	144
parotid gl.	250	64	107	37	n.d.	n.d.	n.d.	n.d.
submand. gl.	275	49	223	45	n.d.	n.d.	n.d.	n.d.

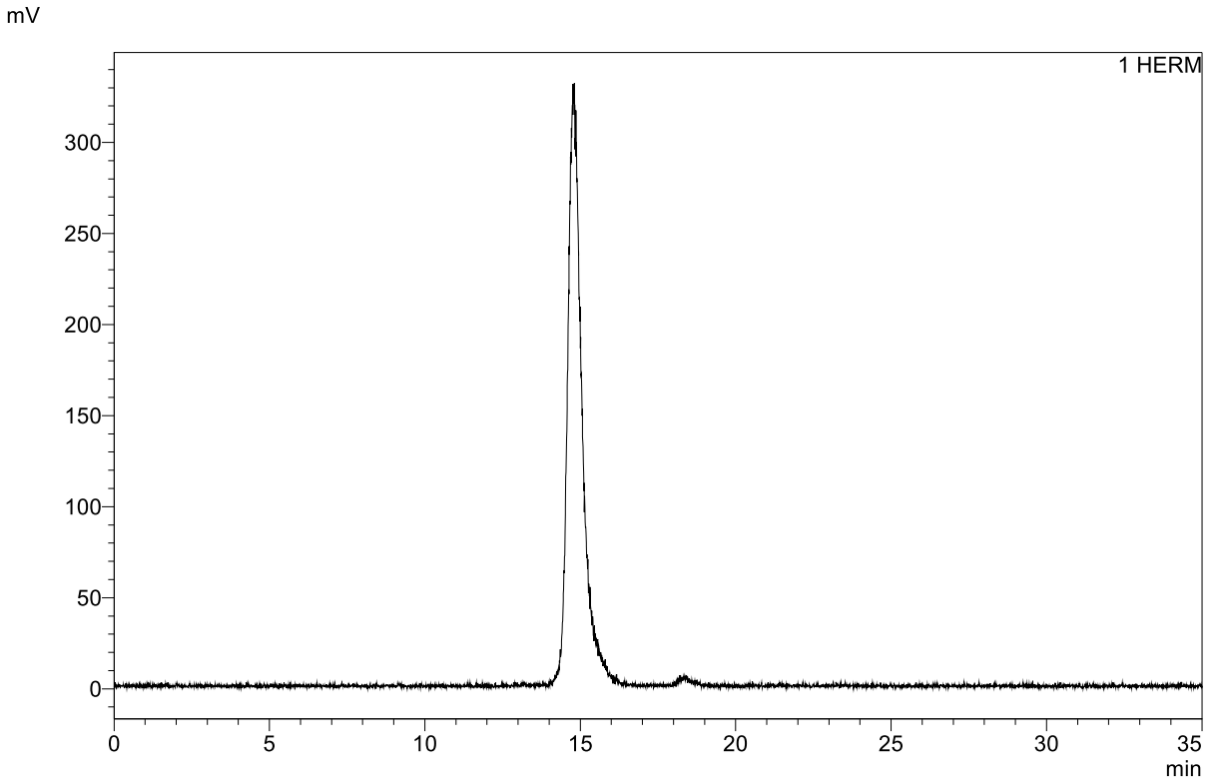

Supplemental Figure 1: Exemplary radio-chromatogram of [^{177}Lu]Lu-rhPSMA-7.3 in the AMSEC experiment. The retention time of 14.8 min measured in this particular experiment correlates with an AMW of 30.3 kDa (AMW of 30.4 ± 0.5 kDa (mean ± SD) for n = 10 independent measurements).

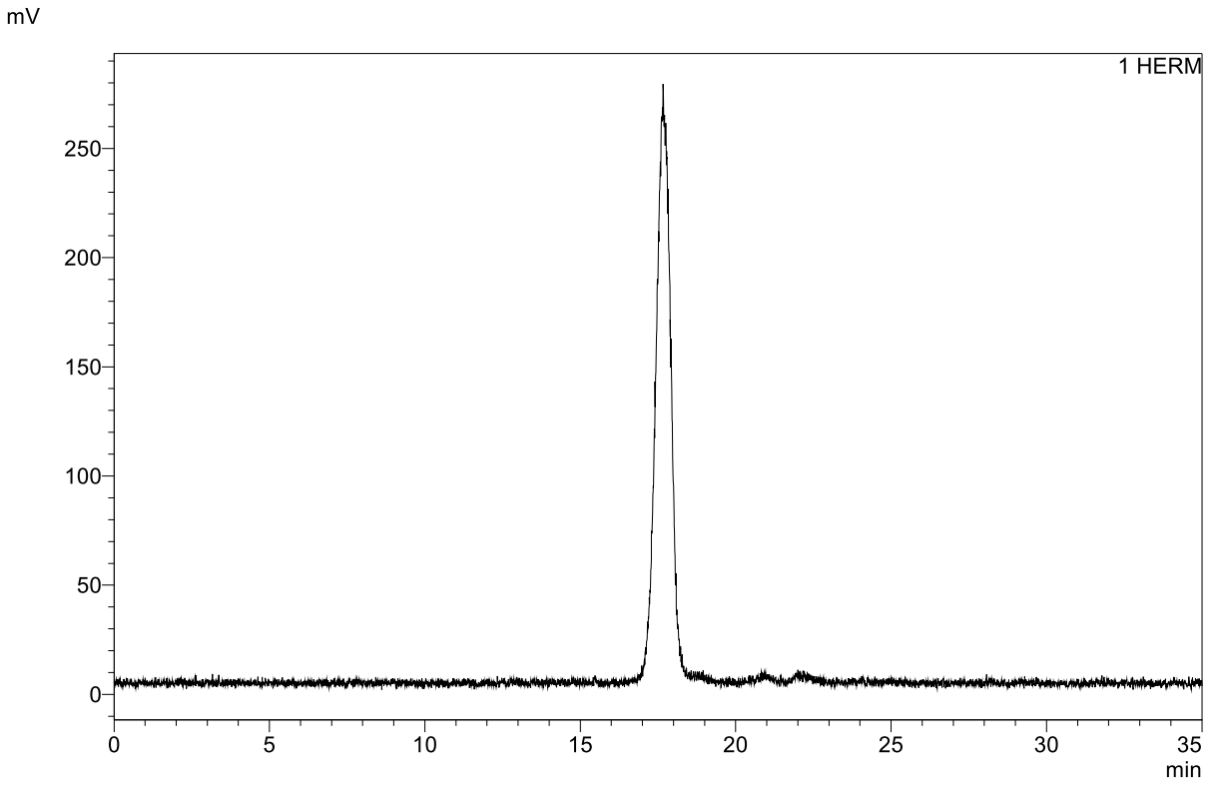

Supplemental Figure 2: Radio-chromatogram of [^{177}Lu]Lu-PSMA-617 in the AMSEC experiment. The retention time of 17.7 min measured in this particular experiment correlates with an AMW of 13.7 kDa.

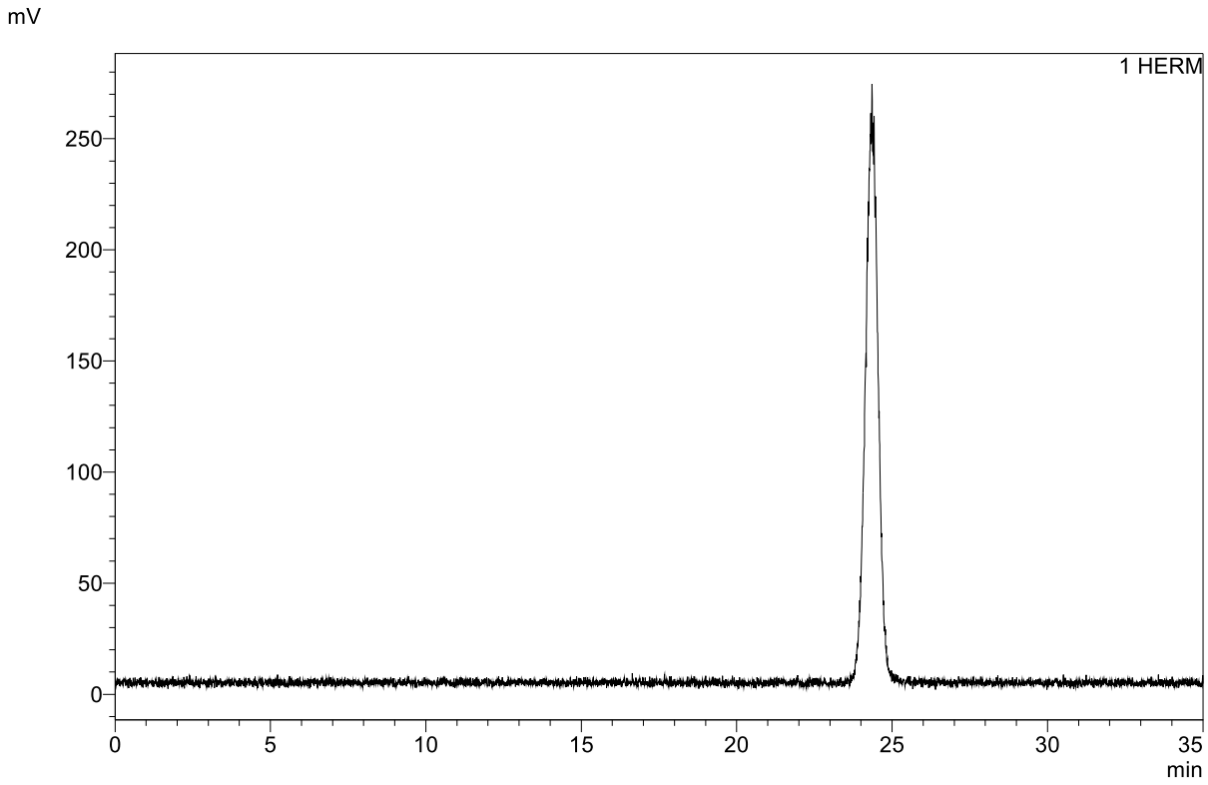

Supplemental Figure 3: Radio-chromatogram of [^{18}F]fluoride in the AMSEC experiment. Due to the absence of interaction of fluoride with HSA, [^{18}F]fluoride is eluted after 24.4 min, as expected for a small inorganic ion, and the corresponding AMW of 2.1 kDa lies below the fractionation range of the gel filtration column (70 – 3 kDa).

References

1. Wurzer A, Parzinger M, Konrad M, et al. Preclinical comparison of four [(18)F, (nat)Ga]rhPSMA-7 isomers: influence of the stereoconfiguration on pharmacokinetics. *EJNMMI Res.* 2020;10:149.

2. Weineisen M, Schottelius M, Simecek J, et al. 68Ga- and 177Lu-Labeled PSMA I&T: Optimization of a PSMA-Targeted Theranostic Concept and First Proof-of-Concept Human Studies. *J Nucl Med.* 2015;56:1169-1176.

3. Wirtz M, Schmidt A, Schottelius M, et al. Synthesis and in vitro and in vivo evaluation of urea-based PSMA inhibitors with increased lipophilicity. *EJNMMI Res.* 2018;8:84.